

The X-ray afterglow of GRB 081109A: clue to the wind bubble structure

Z. P. Jin^{1,2}, D. Xu^{3*}, S. Covino⁴, P. D’Avanzo⁴, A. Antonelli⁵, Y. Z. Fan^{6,1}, D. M. Wei¹

¹*Purple Mountain Observatory, Chinese Academy of Sciences, Nanjing 210008, China*

²*Graduate School, Chinese Academy of Sciences, Beijing, 100012, China*

³*Dark Cosmology Centre, Niels Bohr Institute, University of Copenhagen, Juliane Maries Vej 30, DK-2100, Copenhagen, Denmark*

⁴*INAF / Brera Astronomical Observatory, Via Bianchi 46, 23807, Merate (LC), Italy*

⁵*INAF / Rome Astronomical Observatory, Via Frascati 33, 00044, Monte Porzio (Roma), Italy*

⁶*Niels Bohr International Academy, Niels Bohr Institute, University of Copenhagen, Blegdamsvej 17, DK-2100 Copenhagen, Denmark*

Accepted Received; in original form

ABSTRACT

We present the prompt BAT and afterglow XRT data of *Swift*-discovered GRB 081109A up to $\sim 5 \times 10^5$ sec after the trigger, and the early ground-based optical follow-ups. The temporal and spectral indices of the X-ray afterglow emission change remarkably. We interpret this as the GRB jet first traversing the freely expanding supersonic stellar wind of the progenitor with density varying as $\rho \propto r^{-2}$. Then after approximately 300 seconds the jet traverses into a region of apparent constant density similar to that expected in the stalled-wind region of a stellar wind bubble or the interstellar medium (ISM). The optical afterglow data are generally consistent with such a scenario. Our best numerical model has a wind density parameter $A_* \sim 0.02$, a density of the stalled wind $n \sim 0.12 \text{ cm}^{-3}$, and a transition radius $\sim 4.5 \times 10^{17} \text{ cm}$. Such a transition radius is smaller than that predicted by numerical simulations of the stellar wind bubbles and may be due to a rapidly evolving wind of the progenitor close to the time of its core-collapse.

Key words: Gamma Rays: bursts –GRBs: individual (GRB 081109A)–ISM: jets and outflows–radiation mechanisms: nonthermal

* emails: jin@pmo.ac.cn (ZPJ) and dong@astro.ku.dk(DX)

1 INTRODUCTION

Gamma-ray bursts (GRBs) are the most luminous explosions in the Universe. They feature extremely relativistic outflows with bulk Lorentz factors of 10^{2-3} and isotropic energies of 10^{48-54} ergs. These energies are widely believed to be generated via the core-collapse of massive stars for conventional long(-duration) GRBs (e.g., Woosley 1993; Woosley & Bloom 2006) or the merger of compact star binaries for conventional short(-duration) GRBs (e.g., Eichler et al. 1989; Narayan, Paczyński, & Piran 1992). In the standard fireball model the prompt soft γ -ray emission is powered by the collision of the material shells within the relativistic outflow (i.e., the internal shocks); afterwards these material shells spread and merge into a single uniform outflow, continuing to move outwards; then the long-lived X-ray, optical and radio afterglow emission is powered by the interaction of the overall outflow and the circum-burst medium (e.g., Piran 1999; Mészáros 2002; Zhang & Mészáros 2004). Therefore, the temporal and spectral evolution of the multi-wavelength afterglow can be used to diagnose the underlying radiation mechanism and the profile of the circumburst medium (e.g., Sari, Piran, & Narayan 1998; Chevalier & Li 2000; Panaiteescu & Kumar 2002).

For short GRBs, the circum-burst medium is expected to be of the interstellar medium (ISM) type or even of the intergalactic medium (IGM) type, for which the number density is roughly constant and much lower than unity, being consistent with the current afterglow modeling (see Nakar 2007, for a review). For long GRBs, Panaiteescu & Kumar (2002) found that the afterglow modeling usually favors the constant density (CD) medium scenario, half cases in 10 bursts of a sample were better fitted by the CD medium while only one better described by a free wind (FW) medium. However, Starling et al. (2008) found that in 10 bursts of a sample, 4 were clearly in FW medium while only 1 consistent with CD medium. It seems that the circum-burst environments are unlikely to be drawn from only one of the CD or FW profile for long bursts. This is not obviously consistent with the collapsar model in which an ideal FW circum-burst medium would be created. The FW has a density profile $\rho = 5 \times 10^{11} A_* r^{-2} \text{ g cm}^{-3}$, here $A_* = \left(\frac{\dot{M}}{10^{-5} M_\odot \text{ yr}^{-1}} \right) \left(\frac{1000 \text{ km s}^{-1}}{v_w} \right)$ is the parameter reflecting the density of the wind. One potential solution is that the ideal FW medium profile has been modified before the GRB explosion. As is known, massive stars are believed to enter the Wolf-Rayet stage during their late evolution and have lost a major fraction of their masses in the form of the stellar wind. The interaction between this stellar wind and the surrounding medium creates a bubble structure (e.g., Weaver et al. 1977; Wijers 2001; Ramirez-Ruiz et al. 2001; Dai & Wu 2003; Chevalier, Li & Fransson 2004; van Marle et al. 2006, 2007, 2008; Eldridge et al. 2006; Eldridge 2007; Pe'er & Wijers 2006). In this scenario the free expanding supersonic wind is ter-

minated at a radius $R_t \sim 10^{18} - 10^{20}$ cm, where the density jumps by a factor of 4 or more with the lower value expected for such an adiabatic shock. Beyond the wind termination shock is the roughly constant density stalled wind, holding up to a rather large radius $R_{ISM} \sim 10^{19} - 10^{21}$ cm, outside this radius is the very dense swept-up ISM (the number density $n \sim 10^2 - 10^3$ cm $^{-3}$) and then the ISM.

If the above picture is a good approximation of the circum-burst medium, it may be possible to observe afterglow signatures caused by the medium transition at $\sim R_t$ or even at $\sim R_{ISM}$. In Section 2, we describe the signatures in GRB afterglows for the first transition which is more easily observed and more of interest with respect to the second one. Such a transition is possibly evident in GRB 050319 (Kamble et al. 2007) and GRB 050904 (Gendre et al. 2007). In Section 3, we present the X-ray afterglow observations of GRB 081109A which leads to reach the conclusion that the FW-CD transition is quite clear in this event. The optical afterglow data are generally consistent with such a scenario. Throughout this work we use the notation $F(t, \nu) \propto t^\alpha \nu^\beta$ for the afterglow monochromatic flux as a function of time, where ν represents the observer's frequency, α is the monochromatic flux decay index, and β is the energy spectrum index. The convention $Q_x = Q/10^x$ has been adopted in cgs units.

2 THE AFTERGLOW SIGNATURES OF THE MEDIUM TRANSITION

The GRB afterglow emission in the CD or FW scenarios has been extensively discussed (see Zhang & Meszaros 2004 for a review). We use the standard fireball afterglow theory with the simple microphysical assumptions of constant energy fractions imparted to the swept-up electrons, ϵ_e , and to the generated magnetic field, ϵ_B , respectively. The typical synchrotron radiation frequency ν_m and the cooling frequency ν_c are calculated in the standard way (Sari, Piran, & Narayan 1998). Both scenarios lead to the afterglow closure relations made of the temporal decay index α and the spectral index β , depending upon the spectral segment and the energy distribution index of $p \sim 2 - 3$ of the swept-up electrons. Usually the synchrotron self-absorption frequency, ν_a , is much lower than the optical band and thus neglected unless radio observation invoked. Therefore, with good-quality temporal and spectral data, the circum-burst medium profile can be reliably constrained. We summarize the closure relation in Table 1 apart from the $\nu < \nu_a$ cases (see also Pe'er & Wijers 2006).

For the X-ray afterglow of our interest, there are two ways to diagnose the number density profile of the medium:

Table 1. Temporal index α and spectral index β in the cases that the medium profile can be constrained, where the convention $F(t, \nu) \propto t^\alpha \nu^\beta$ is adopted, p is the power-law index of the swept-up electrons, and ν_a , ν_c , and ν_m are the self-absorption frequency, the cooling frequency and the characteristic frequency in the synchrotron radiation, respectively (Sari, Piran, & Narayan 1998; Chevalier & Li 2000).

Case	β	α (CD)	α (FW)
$\nu_a < \nu < \nu_c < \nu_m$	1/3	1/6	-2/3
$\nu_a < \nu < \nu_m < \nu_c$	1/3	1/2	0
$\max\{\nu_a, \nu_m\} < \nu < \nu_c$	$-\frac{p-1}{2}$	$\frac{3-3p}{2}$	$\frac{1-3p}{2}$
$\nu_c < \nu$	$-\frac{p}{2}$	$\frac{2-4-3p}{4}$	$\frac{2-4-3p}{4}$

(I) When $\nu_m < \nu_{\text{opt}} < \nu_c < \nu_X$ occurs, in the FW scenario the X-ray emission drops with time as $t^{(2-3p)/4}$ while the optical emission drops faster by a factor of 1/4. On the contrary, in the CD scenario the optical emission drops more slowly than the X-rays.

(II) In the case of $\nu_m < \nu_X < \nu_c$, i.e., the X-ray emission is in the slow cooling phase, the temporal and spectral indices roughly satisfy $\alpha = (3\beta - 1)/2$ in the FW scenario.

Then how does the afterglow evolve after the FW-CD transition at the radius R_t ? It is known that the characteristic frequency ν_m decays with time as $t^{-3/2}$ in both CD and FW scenarios. However, the cooling frequency ν_c evolves very differently. In the FW scenario it increases as $t^{1/2}$ but in the CD scenario it declines as $t^{-1/2}$. Therefore, the following observational signatures would be evident before and after the transition. In Case I, the deceline of the X-ray emission remains unchanged while the optical decay becomes shallower by a factor of $t^{1/2}$ as long as the optical band is still below ν_c . In Case II, the X-ray decay will get flattened by a factor of $t^{1/2}$ as long as the X-ray band is still below ν_c . Afterwards, when ν_c drops below the X-ray band, the X-ray decay steepens by a factor of $t^{-1/4}$. As we'll show in next Section, the X-ray afterglow of GRB 081109A fits Case II.

3 THE FW-CD TRANSITION IN GRB 081109A

3.1 Observation and data reduction of GRB 081109A

GRB 081109A was triggered and located by Burst Alert Telescope (BAT) onboard *Swift* at 07:02:06 UT (trigger 334112), November 9th, 2008 (see Immler et al. 2008). We downloaded the raw data from the UK *Swift* data archive and processed them in a standard way with HEAsoft 6.6. The BAT lightcurve in the 15-350 keV band was processed with the `batgrbproduct` task. This burst has a T_{90} about 61 seconds in 15-350 keV, classified as a long GRB. The duration value is consistent with the duration measurement of 45 s in 8-1000 keV by the Gamma-ray Burst Monitor (GBM) onboard *Fermi* (von Kienlin et al. 2008). Also the time-averaged GBM spectrum is best fit by a

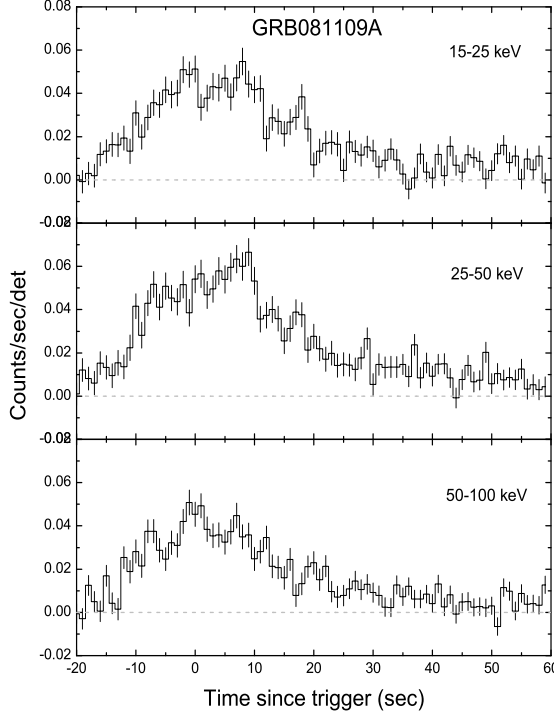


Figure 1. The prompt lightcurves of GRB 081109A in 15-25, 25-50, 50-100 keV with 1 s binning. Spectral lag between different energy bands cannot be well measured for this event due to relatively low signal to noise.

power-law function with an exponential high energy cutoff. The power law index is -1.28 ± 0.09 and the cutoff energy, parameterized as E_p is 240 ± 60 keV (chi squared 510 for 478 d.o.f.). The fluence in 8-1000keV is $6.35 \pm 0.43 \times 10^{-6}$ erg \cdot cm $^{-2}$. Fig. 1 shows the prompt lightcurves of GRB 081109A in 15-25, 25-50, 50-100 keV with 1 s time binning. Spectral lag between different energy bands cannot be well measured for this event due to relatively low signal to noise.

The *Swift* X-ray Telescope (XRT) observations began at 65.6 seconds after the BAT trigger and discovered a bright and fading X-ray afterglow. Observations continued during the following hours and days and in several return visits, with Windowed Timing (WT) mode for ~ 300 s after the trigger and Photon Counting (PC) mode afterwards. Throughout the X-ray observation, spectral softening is evident. There is no need for pile-up correction to WT data as the highest count rate is less than ~ 150 count s $^{-1}$, but such correction should be applied to early PC data when the count rate is higher than ~ 0.6 count s $^{-1}$ in order to get correct X-ray lightcurve and spectra. We made this correction by fitting a King function profile to the point spread function (PSF) to determine the radial point at which the measured PSF deviates from the model. The counts were extracted using an annular aperture that excluded the affected ~ 4 pixel core of the PSF, and the count rate was

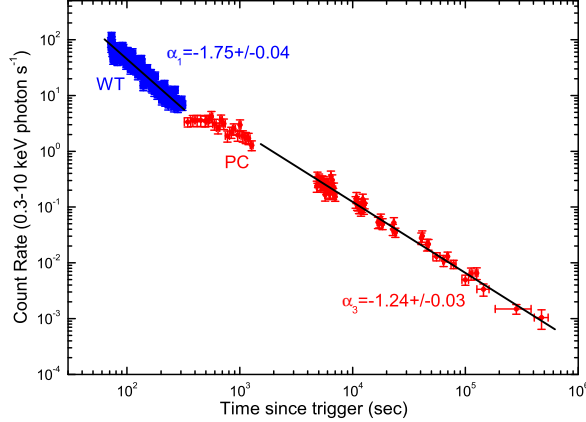


Figure 2. The X-ray afterglow lightcurve of GRB 081109A in 0.3-10 keV. Also marked are the fitting temporal indices for the WT and late PC segments of the lightcurve.

corrected according to the model. We also considered the most recent calibration and exposure maps. Fig. 2 shows the 0.3-10 keV X-ray lightcurve, which can be well modeled with a doubly broken power-law which is equivalent with a broken power-law with a jump transition at ~ 500 s. For a doubly broken power-law, the fitted parameters are: $\alpha_1 = -1.75 \pm 0.04$ ($\chi^2 = 152.4$ for 119), $t_{b1} \sim 310$ s, $\alpha_2 = -0.70 \pm 0.13$ ($\chi^2 = 13.7$ for 18), $t_{b2} \sim 2.9 \times 10^3$ s, $\alpha_3 = -1.24 \pm 0.03$ ($\chi^2 = 38.9$ for 54). The integrated spectra of the above first and third segments are shown in Fig. 3. In detail, the spectral power-law indices are $\beta_1 = -0.74 \pm 0.05$, $\beta_3 = -1.27 \pm 0.10$, and β_2 is in the middle.

The *Swift* Ultraviolet and Optical Telescope (UVOT) began observing at ~ 150 s after the trigger and found no optical counterpart down to ~ 18 mag (Immler et al. 2008). Ground-based observations of the afterglow of GRB 081109A were carried out with the REM telescope at La Silla (Zerbi et al 2001; Chincarini et al 2003; Covino et al. 2004) equipped with the ROSS optical spectrograph/imager and the REMIR near-infrared camera on 2008 Nov 09, starting about 52 seconds after the burst (D'Avanzo et al. 2008). The night was clear, with a seeing of about $2.0''$. We collected images with typical exposures times from 10 to 120 seconds, covering a time interval of about 0.5 hours. Image reduction was carried out by following the standard procedures. Astrometry was performed using the USNOB1.0¹ and the 2MASS² catalogues. We performed aperture photometry for the afterglow and comparison stars. The afterglow was not detected in the optical. In the NIR it was detected only in the *H* and *Ks* bands. Results for the photometry are reported

¹ <http://www.nofs.navy.mil/data/fchpix/>

² <http://www.ipac.caltech.edu/2mass/>

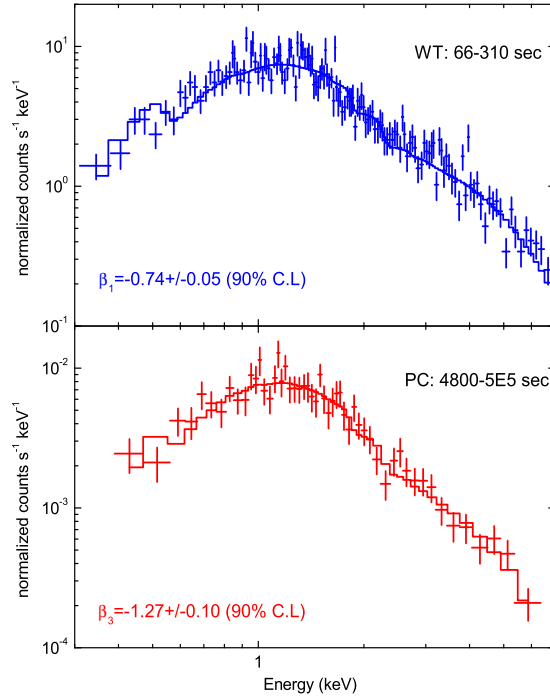


Figure 3. The spectra of the WT and late PC segments of the X-ray afterglow of GRB 081109A. An absorbed power-law fitting is adopted. Also marked are the fitting spectral indices respectively.

Table 2. Optical photometry for GRB 081109A. Upper limits are at 3σ confidence level.

Filter	Time since trigger (s)	Time integral (s)	Magnitude
H	89.4	71.3	>15.0
H	168.9	72.2	15.017 ± 0.115
H	248.4	71.3	>15.4
H	327.0	71.3	14.893 ± 0.109
H	394.4	47.3	14.747 ± 0.128
H	636.3	71.3	14.963 ± 0.114
H	990.6	121.1	>15.5
H	1545.3	171.7	15.763 ± 0.101
K	450.6	45.6	14.365 ± 0.259
K	718.4	72.2	14.465 ± 0.207
K	1122.8	121.1	14.645 ± 0.188

in Table 2. The GROND instrument equipping the 2.2m ESO/MPI telescope at La Silla started observation 17.1 hr after the trigger, gave a redshift limit of $z < 3.5$ and a best fit of intrinsic extinction of Av between 0.6 and 1.2 (Clemens, Kruehler, & Greiner 2008).

3.2 Analytical investigation of the afterglow of GRB 081109A

For $t < t_{b1}$, the temporal index $\alpha_1 = -1.75 \pm 0.04$ and the spectral index $\beta_1 = -0.74 \pm 0.05$ are related by $\alpha - 3\beta/2 \approx -0.5$, being consistent with the forward-shock emission in the FW medium as long as $\nu_m < \nu_x < \nu_c$. For $t > t_{b2}$, the temporal index $\alpha_3 = -1.24 \pm 0.03$ and the spectral index $\beta_3 = -1.27 \pm 0.10$ are related by $\alpha - 3\beta/2 \sim 0.5$, suggesting that the medium can be either FW or CD given $\nu_x > \max\{\nu_m, \nu_c\}$ (Zhang & Mészáros 2004). If the FW scenario holds from the very beginning, we have $\nu_c(t_{b2}) > \nu_c(t_{b1}) > \nu_x$ because of $\nu_c \propto t^{1/2}$. One can, of course, assume that either A_* or ϵ_B has increased abruptly and then get a $\nu_c(t_{b2}) \ll \nu_c(t_{b1})$. However, such a treatment is lack of any solid physical background and is thus artificial. On the other hand, if we assume that at $t \sim t_{b1}$ there comes the FW to CD transition, the forward shock emission light curve will get flattened by a factor of $t^{1/2}$, roughly consistent with the data (please note that α_2 is only poorly constrained). In this scenario, the steepening at $t \geq t_{b2}$ implies that $\nu_c(t_{b2}) > \nu_x$. Below we present our quantitative estimates.

In a FW medium, we have $\alpha_1 = \frac{1-3p}{4}$ and $\beta_1 = -\frac{p-1}{2}$ in the case of $\nu_m < \nu_x < \nu_c$. In a CD medium, we have $\alpha_3 = \frac{2-3p}{4}$ and $\beta_3 = -\frac{p}{2}$ for $\nu_x > \max\{\nu_m, \nu_c\}$. We find that $p = 2.5$ fits both the temporal and spectral slopes of GRB 081109A.

In a FW medium, we have (e.g., Chevalier & Li 2000):

$$F_{\nu, \text{max}} = 0.23 \text{ Jy } D_{\text{L}, 28.34}^{-2} \epsilon_{\text{B}, -2}^{1/2} E_{\text{k}, 53}^{1/2} A_* t_{\text{d}, -3}^{-1/2}, \quad (1)$$

$$\nu_m = 1.8 \times 10^{16} \text{ Hz } C_p^2 \left(\frac{1+z}{2}\right)^{1/2} \epsilon_{\text{e}, -1}^2 \epsilon_{\text{B}, -2}^{1/2} E_{\text{k}, 53}^{1/2} t_{\text{d}, -3}^{-3/2}, \quad (2)$$

$$\nu_c = 1.1 \times 10^{13} \text{ Hz } \left(\frac{1+z}{2}\right)^{-3/2} \epsilon_{\text{B}, -2}^{-3/2} E_{\text{k}, 53}^{1/2} A_*^{-2} t_{\text{d}, -3}^{1/2}, \quad (3)$$

where E_k is the isotropic equivalent energy, z is the redshift of the GRB and D_L is the corresponding luminosity distance, t_d is the time in days since trigger in the observer's frame, and $C_p \equiv 13(p-2)/[3(p-1)]$.

In our model, at $t \sim 65.6$ s, $\nu_m < 0.3\text{keV}$, $\nu_c > 10\text{keV}$ and $F_{0.3\text{keV}} \sim 2.6 \times 10^{-3}$ Jy are needed. So we have

$$\epsilon_{\text{e}, -1}^4 \epsilon_{\text{B}, -2} E_{\text{k}, 53} < 3 \quad (\nu_m < 0.3\text{keV}), \quad (4)$$

$$\epsilon_{\text{B}, -2}^{3/4} E_{\text{k}, 53}^{-1/4} A_* < 0.002 \quad (\nu_c > 10\text{keV}), \quad (5)$$

$$\epsilon_{\text{e}, -1}^{3/2} \epsilon_{\text{B}, -2}^{7/8} E_{\text{k}, 53}^{7/8} A_* \sim 0.01. \quad (6)$$

In a CD medium, we have (e.g., Sari, Piran, & Narayan 1998):

$$F_{\nu, \text{max}} = 6.6 \text{ mJy } \left(\frac{1+z}{2}\right) D_{\text{L}, 28.34}^{-2} \epsilon_{\text{B}, -2}^{1/2} E_{\text{k}, 53} n_0^{1/2}, \quad (7)$$

$$\nu_m = 2.4 \times 10^{16} \text{ Hz } C_p^2 \left(\frac{1+z}{2}\right)^{1/2} \epsilon_{e,-1}^2 \epsilon_{B,-2}^{1/2} E_{k,53}^{1/2} t_{d,-3}^{-3/2}, \quad (8)$$

$$\nu_c = 4.4 \times 10^{16} \text{ Hz } \left(\frac{1+z}{2}\right)^{-1/2} \epsilon_{B,-2}^{-3/2} E_{k,53}^{-1/2} n_0^{-1} t_{d,-3}^{-1/2}, \quad (9)$$

where n is the density of CD medium.

At $t \sim t_{b2} \sim 2900$ s, our model suggests that ν_m and $\nu_c < 0.3\text{keV}$, and $F_{0.3\text{keV}} \sim 5.7 \times 10^{-5}$ Jy.

We then have

$$\epsilon_{e,-1}^4 \epsilon_{B,-2} E_{k,53} < 8 \times 10^4 \quad (\nu_m < 0.3\text{keV}), \quad (10)$$

$$\epsilon_{B,-2}^3 E_{k,53} n_0^2 > 0.01 \quad (\nu_c < 0.3\text{keV}), \quad (11)$$

$$\epsilon_{e,-1}^{3/2} \epsilon_{B,-2}^{1/8} E_{k,53}^{9/8} \sim 1.8. \quad (12)$$

In a termination shock model, the crossing time is estimated by Chevalier, Li & Fransson (2004):

$$t(R_t) = 1.5h \left(\frac{1+z}{2}\right) E_{k,53}^{-1} A_{*, -1}^2 n_0^{-1} \sim 310\text{s}, \quad (13)$$

i.e.,

$$E_{k,53}^{-1} A_{*, -1}^2 n_0^{-1} \sim 0.06. \quad (14)$$

For GRB 081109A, there is no self-consistent solution for Eqs.(4-6), Eqs.(10-12) and Eq.(14) provided that ϵ_B is a constant in the free wind and in the CD medium. With eqs.(14), (5) and (11), we have $\epsilon_{B,CD}/\epsilon_{B,w} \geq 7$, where the subscripts “CD” and “w” represent the physical parameters measured in CD and FW medium, respectively. A similar assumption was needed in the modeling of the afterglow data of GRB 050904 (Gendre et al. 2007) and GRB050319 (Kamble et al. 2007). The physical reason is that the CD medium has been heated by the termination reverse shock and then may be weakly magnetized.

The optical data, though rare comparing with the X-ray ones, provide us a reliable test of the current afterglow model. As shown in Fig.4, the H-band lightcurve is distinguished by a flat at early time and then a re-brightening at $t \sim 400$ s. These features are generally consistent with our FW to CD medium model. In the FW medium, a flat segment is expected if the observer’s frequency ν_{obs} is above the synchrotron self-absorption frequency ν_a but below $\nu_m (< \nu_c)$. In the CD medium, a re-brightening is present if the relation $\nu_a < \nu_{\text{obs}} < \nu_m < \nu_c$ still holds (e.g., Zhang & Mészáros 2004). The re-brightening peaks when ν_m crosses the observer’s frequency.

After then the flux will drop with time as $t^{3(1-p)/4}$, a little bit shallower than the simultaneous X-ray decline, as suggested by the H-band data.

3.3 Numerical fit of the afterglow of GRB 081109A

The code used here to fit the X-ray light curves has been developed by Yan, Wei & Fan (2007), with small changes to adapt a density transition in surrounding medium. Assuming a FW to CD medium transition, we find out that the observation data can be reasonably reproduced with the following parameters (see Fig. 4 and Fig. 5): $E_k = 4 \times 10^{54}$ erg, the initial Lorentz factor $\gamma_0 = 500$, $A_* = 0.02$, $n = 0.12 \text{ cm}^{-3}$, $R_t = 4.5 \times 10^{17} \text{ cm}$, $\epsilon_e = 0.02$, $p = 2.5$, $\epsilon_{B,w} = 0.0002$ and $\epsilon_{B,CD} = 0.001$. The source is assumed to be at a redshift $z = 1$. As shown in Fig. 5, a sudden increase of ϵ_B for $t \geq t_{b1}$ is required to account for the jump of ν_c inferred from the X-ray data. $A_* \sim 0.01$ and $R_t \sim 10^{17} - 10^{18} \text{ cm}$ is lower than the typical value found in numerical simulations and may be due to a rapidly evolving wind of the progenitor close to the time of its core-collapse (Eldridge et al. 2006; Eldridge 2007; van Marle et al. 2008). Assuming a redshift $z = 1$, the isotropic energy E_γ in the energy range of 1 – 10000 keV is about 5×10^{52} ergs. The corresponding GRB efficiency $E_\gamma/(E_\gamma + E_k)$ is $\sim 1\%$. Such a low efficiency, though not typical, is still reasonable, as found in previous estimates (e.g., Fan & Piran 2006; Jin & Fan 2007).

The observed optical flux is lower than the value extrapolated from X-ray observation, which implies that there is extinction in optical band. To agree with the optical observation, our numerical fit for the H and Ks band has been adjusted by a factor of 0.3, which requires about 1 mag extinction caused by the GRB host galaxy at the observed H and Ks band. They are about 1 micron at the GRB host galaxy. It essentially means $E_{B-V} \sim 0.8 - 0.9$ assuming Milky Way or SMC extinction curves. With a Galactic dust to gas ratio it would correspond to $N_H \sim 5 \times 10^{21} \text{ cm}^{-2}$. The fit is shown in Fig. 4. The small differences around the termination radius may due to the sharp density jump we have assumed.

Before the blast wave reaches R_t , its radius can be estimated as (Chevalier & Li 2000):

$$R = 3.5 \times 10^{17} \left(\frac{1+z}{2} \right)^{-1/2} E_{k,53}^{1/2} A_*^{-1/2} t_d^{1/2} \text{ cm.} \quad (15)$$

For $t(R_t) \sim 310$ s, with eq.(5) we have $R = R_t \geq 10^{22} [(1+z)/2]^{-1/2} A_*^{3/2} \epsilon_{B,-2}^{3/2} \text{ cm}$. This implied that R_t depends on the undetermined redshift z weakly. A larger A_* requires a smaller $\epsilon_{B,w}$ otherwise R_t will be much smaller than a few $\times 10^{17}$ cm, the lowest value expected in the numerical simulation. Since the derived $\epsilon_{B,w}$ is already as low as $\sim 10^{-4}$, a smaller value is less likely. That is why we will not consider the case of a FW parameter $A_* \gg 0.01$.

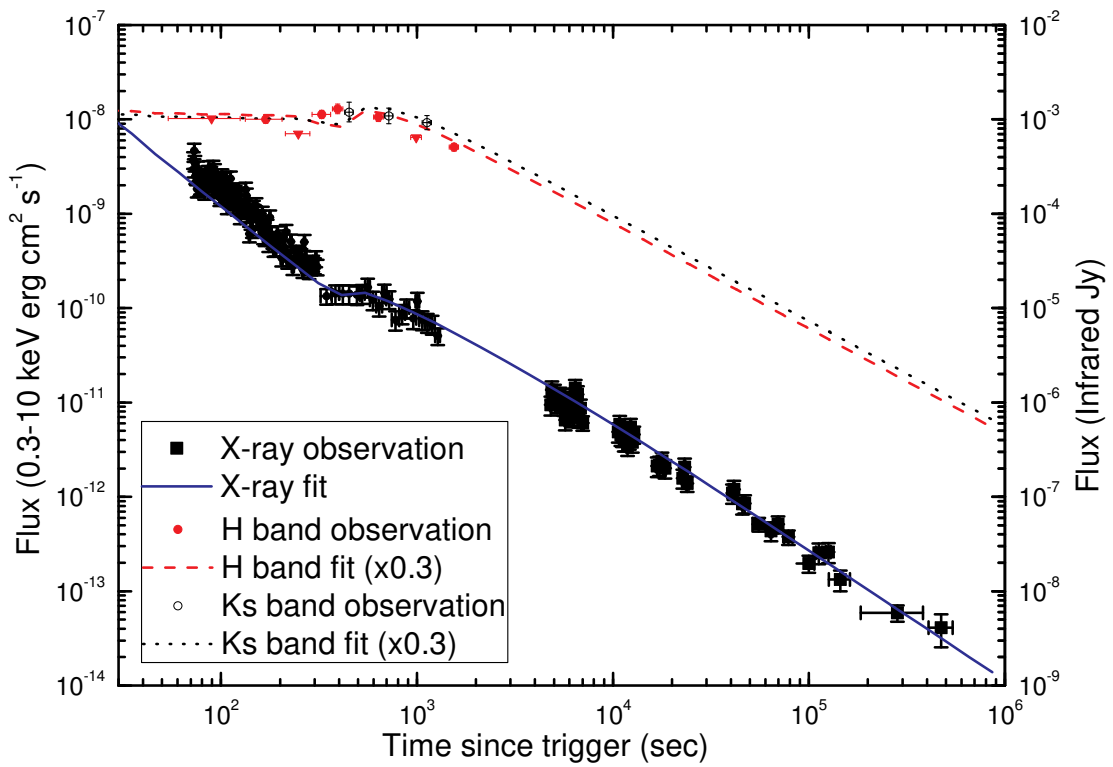


Figure 4. Numerical fit to the afterglow of GRB081109A. The solid circles and squares are X-ray observations, and the solid line is our numerical fit to X-ray. The circles on the top are H band (empty) and Ks band (solid) observations, the triangles are upper limits in H band. The dashed and dotted lines are numerical fit to H band and Ks band data, respectively.

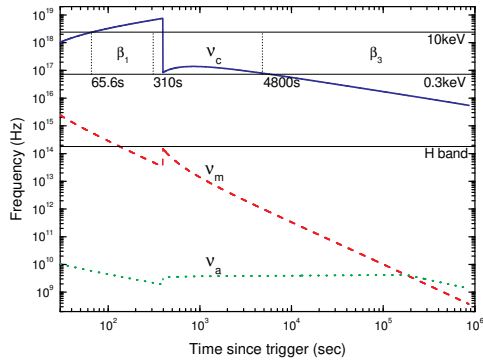


Figure 5. Numerical fit to the spectrum evolution in GRB081109A afterglow. In the X-ray band(0.3-10keV), the spectrum between 65.6s and 310s is a single power law $\beta_1 = 0.75$, and after ~ 4800 s is another single power law $\beta_3 = 1.25$.

When a GRB jet finally enters into the very dense swept-ISM region, strong reverse shock may be formed and an afterglow re-brightening is expected (Dai & Wu 2003; Pe'er & Wijers 2006). The X-ray observation for GRB081109A lasted to about 4.7×10^5 s after the trigger and did not find obvious flux enhancement. In our numerical fit, the jet front reached a radius $\sim 1.9 \times 10^{18}$ cm at such a late time, much smaller than R_{ISM} estimated by numerical simulations (Eldridge et al. 2006; Eldridge 2007). So the GRB outflow was still in the shocked wind material ejected in the Wolf-Rayet stage with an approximately constant density (Weaver et al. 1977).

4 CONCLUSION AND DISCUSSION

Although some GRBs are inferred to occur in free stellar wind medium (e.g., Panaiteescu & Kumar 2002; Starling et al. 2008), most are inferred to occur in a medium with a constant number density (even for some bursts associated with bright supernovae, see Fan 2008, and the references therein), which may indicate that GRB outflows expand into the wind bubble rather than the ideal free stellar wind. As shown in Section 2 of this work, in some cases the X-ray afterglow data could shed light on the wind bubble structure. Therefore the X-ray afterglow observation since the early time is required to trace the profile of the circum-burst medium. However, in many *Swift* GRB events the early X-ray afterglow deviates from the standard afterglow model significantly (Nousek et al. 2006; Zhang et al. 2006). For instance, the prolonged activity of GRB central engines would generate energetic X-ray flares that have outshone the regular forward shock emission (e.g., Fan & Wei 2005; Zhang et al. 2006; Nousek et al. 2006). Fortunately, in GRB 081109A there is no flare accompanying the early X-ray afterglow. The temporal and spectral evolutions of the X-ray afterglow imply a medium transition at the radius $R_t \sim 4.5 \times 10^{17}$ cm (see Section 3). Such a small R_t implies a small wind parameter A_* and a large p/k since

$$R_t = 5.7 \times 10^{17} \left(\frac{v_w}{10^3 \text{ km s}^{-1}} \right) \left(\frac{p/k}{10^6 \text{ cm}^3 \text{ K}} \right)^{-1/2} A_{*, -2}^{1/2} \text{ cm},$$

where p is the pressure in the shocked wind and k is the Boltzmann constant (Chevalier, Li & Fransson 2004). Indeed A_* is found to be as small as 10^{-2} in our numerical fit. GRB 081109A is thus a good candidate of long GRBs born in wind bubble.

The rising behavior of the very early afterglow lightcurves can play an important role in probing the density profile of the medium. This is particularly the case if the reverse shock optical emission is very weak. As shown in Jin & Fan (2007) and Xue et al. (2009), in the free wind scenario the very early optical rise is usually not expected to be faster than $t^{1/2}$ while in the constant density medium the rise can be faster than t^2 . Therefore the $\sim t^3$ -like rise in the

early optical/infrared/X-ray afterglows of GRB 060418, GRB 060607A (Molinari et al. 2007), GRB 060801, GRB 060926, GRB 080319C, and GRB 080413B (Xue et al. 2009) rules out the free wind medium for $R > 10^{16}$ cm. Thus the absence of the free wind signature in some GRB afterglows is still a puzzle. One possible solution is that the mass loss rate due to the stellar wind before massive stars collapse is not a constant and might be much lower than previously assumed (Eldridge et al. 2006; Eldridge 2007).

ACKNOWLEDGMENTS

We would like to thank the referee for the constructive comments and for the help in improving the presentation of this work. This work is supported by the National Science Foundation (grants 10673034 and 10621303) and National Basic Research Program (973 programs 2007CB815404 and 2009CB824800) of China. DX is at the Dark Cosmology Centre funded by Danish National Research Foundation. YZF is also supported by Danish National Research Foundation and by Chinese Academy of Sciences.

REFERENCES

Chevalier, R. A., Li, Z. Y., 2000, ApJ, 536, 195
 Chevalier, R. A., Li, Z. Y., Fransson, C., 2004, ApJ, 606, 369
 Chincarini, G., Zerbi, F. M., Antonelli, A. et al. 2003, The Messenger, 113, 40
 Clemens, C., Kruehler, T., Greiner, J., 2008, GCN Circ., 8515
 Covino, S., Stefanon, M. Fernandez-Soto, A. et al. 2004, SPIE 5492, 1613
 D'Avanzo, P., Covino, S., Antonelli, L.A. et al. 2008, GCN 8501
 Dai, Z. G., Wu, X. F., 2003, ApJ, 591, L21
 Eichler, D., Livio, M., Piran, T., Schramm, D. N., 1989, Nat, 340, 126
 Eldridge, J. J. et al., 2006, MNRAS, 367, 186
 Eldridge, J. J., 2007, MNRAS, 377, L29
 Fan Y. Z., 2008, MNRAS, 389, 1306
 Fan Y. Z., Piran T., 2006, MNRAS, 369, 197
 Fan Y. Z., Wei D. M., 2005, MNRAS, 364, L42
 Gendre, B. et. al., 2007, A&A, 462, 565
 Immler, S. et al., 2008, GCN Circ., 8500
 Jin Z. P., Fan Y. Z., 2007, MNRAS, 378, 1043

Kamble, A., Resmi, L., Misra, K., 2007, *ApJ*, 664, L5

Mészáros, P., 2002, *ARA&A*, 40, 137

Molinari, E. et al., 2007, *A&A*, 469, L13

Nakar, E., 2007, *Phys. Rep.*, 442, 166

Narayan, R., Paczyński, B., Piran, T., 1992, *ApJ*, 395, L83

Nousek, J. A. et al., 2006, *ApJ*, 642, 389

Panaitescu, A., Kumar, P., 2002, *ApJ*, 571, 779

Pe'er, A. & Wijers, R. A. M. J., 2006, *ApJ*, 643, 1036

Piran, T., 1999, *Phys. Rep.*, 314, 575

Ramirez-Ruiz, E., Dray, L. M., Madau, P., Tout, C. A., 2001, *MNRAS*, 327, 829

Sari, R., Piran, T., Narayan, R., 1998, *ApJ*, 497, L17

Starling et al., 2008, *ApJ*, 672, 433

van Marle, A. J., Langer, N., Achterberg, A., Garcia-Segura, G., 2006, *A&A*, 460, 105

van Marle, A. J., Langer, N., García-Segura, G., 2007, *A&A*, 469, 941

van Marle, A. J., Langer, N., Yoon, S.-C., García-Segura, G., 2008, *A&A*, 478, 769

von Kienlin, A., 2008, *GCN Circ.* 8505

Weaver, R., McCray, R., Castor, J., Shapiro, P., Moore, R., 1977, *ApJ*, 218, 377

Wijers, R. A. M. J., 2001, Gamma-Ray Bursts in the Afterglow Era:Proceedings of the International Workshop Held in Rome, Italy, 17-20 October 2000, ESO ASTROPHYSICS SYMPOSIA. Edited by E. Costa, F. Frontera, and J. Hjorth. Springer-Verlag,306

Woosley, S., 1993, *ApJ*, 405, 273

Woosley, S. E., Bloom, J. S., 2006, *ARA&A*, 44, 507

Xue, R. R., Fan, Y. Z., Wei, D. M., 2009, *A&A*, 498, 671

Yan, T., Wei, D. M., Fan, Y. Z., 2007, *Chin. J. Astron. Astrophys.*, 7, 777

Zerbi, F. M., Chincarini, G., Ghisellini, G. et al. 2001, *AN* 322, 275

Zhang, B. et al. 2006, *ApJ*, 642, 354

Zhang, B., Mészáros, P., 2004, *IJMPA*, 19, 2385